A nesting approach for the numerical analysis of MRI birdcage antennas in the presence of the human head

Farzad Jabbarigargari[1], Chan-Sun Park[1], Donia Oueslati[1], Denis Tihon[2], Clément Durochat[3], Thibaut Letertre[4], Pierre Sabouroux[4], Christophe Craeye[1]

[1] Universite catholique de Louvain: ICTEAM, Louvain-la-Neuve, Belgium, farzad.jabbarigargari@uclouvain.be
[2]Cavendish Laboratory, University of Cambridge, Cambridge, UK
[3]Multiwave Imaging SAS, Marseille, France
[4]Aix Marseille Univ., CNRS, Centrale Marseille, Institut Fresnel, Marseille, France

***Abstract*—Integral-equation approaches are among the solvers that can be used to analyse RF fields in MRI scanners, in particular when the human body is divided into a collection of homogeneous objects. This solver can be relatively intensive in terms of computation time and memory if the full solution is rerun everytime minor changes are considered in the MRI antennas. In this work, an efficient solving tool based on a nesting approach is proposed. The idea consists of avoiding re-computation of all the equivalent currents inside the body. A validation is provided for a simple structure with a commercial solver (CST); then by using a developed in-house code, the magnetic field inside the brain is shown when a birdcage antenna is used around the human head.**

***Index Terms*—antennas, magnetic resonance imaging, nesting appraoch, method of moments.**

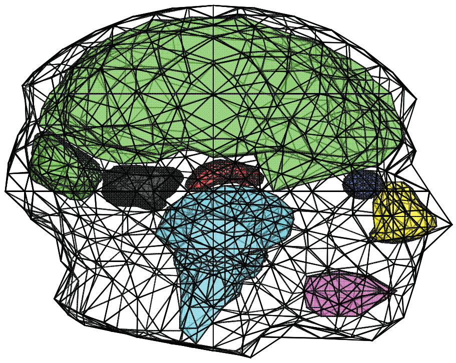

Fig. 1. A meshed human head with several internal organs.

I. Introduction

Magnetic resonance imaging (MRI) is a powerful, non invasive technique to form images of human or animal body, based on the interaction between RF fields and hydrogen atoms [1],[2]. The signal-to-noise ratio (SNR) has been improved by increasing the amount of magnetic flux density, B_0, from 1 Tesla at first [3] to 11.7 Tesla for nowadays applications that can be used for the human body [4]. The working frequency of the MRI, ω_0, is proportional to the magnetic flux density. Hence at high and ultra-high magnetic field strengths, the wavelength becomes equal or even smaller than the effective dimension of the human body, which will affect specific absorption rate (SAR), the homogeneity of magnetic field and images quality [5]. So it is necessary to use effective and reliable solvers to find the fields distribution inside a desired medium. In this case numerical methods can be used to find fields in the UHF band for a given distribution of materials (human body, supporting structures, MRI tunnel and antennas themselves), and a given excitation of the antennas. Such a field representation allows one to check (i) that the magnetic fields have the proper homogeneity, so as to allow imaging with homogeneous signal-to-noise ratio, (ii) that the electric field does not reach too high values, so as to avoid a too high SAR and (iii) that the power provided by the generators does not get reflected towards them (impedance matching). Two categories of methods exist, depending on the fact that fields are explicitly written as radiated by sources distributed over certain surfaces or volumes or, alternatively, as satisfying locally the relations between their derivatives versus space (and also time in the non-harmonic case) [6]- [10]. The choice is essentially application-driven. The integral-equation approaches are preferred when the media are piecewise homogeneous. This is true in general for man-made objects, such as antennas, MRI tunnels and metamaterials. That is only partially true for the human body. Nevertheless, it is possible to distinguish between different types of materials: bone, fat, brain, muscle, etc. Recently a method which is based on the volumetric integral equations has been proposed to accelerate the computation time, but despite acceleration, this method is still intensive [11]. The important advantages of surface-integral approaches are twofold. First, unknowns are limited to interfaces between piecewise homogeneous media. Second, there is no need to introduce absorbing conditions at the boundary of the computational domain. The main challenge in integral-equation solvers is that these techniques could be relatively intensive and time consuming if full solution is rerun every time minor changes are considered in the antennas or in the metamaterials that are used in the MRI.

In this work, an efficient and accurate technique is presented for MRI systems. The nesting approach is employed to significantly reduce the computation time in finding electromagnetic (EM) fields inside the desired organ. Assuming that the human head can be considered as a composition of several homogeneous internal organs, as shown in Fig. 1, a nesting approach is used as an integral-equation solver to observe fields inside the brain. The remainder of this paper is organized as follows. In Section II, the surface integral approaches are presented, followed by the nesting approach in Section III. In Section IV, a validation is provided. Perspectives and the conclusion are discussed in Sections V and VI respectively.

II. SURFACE INTEGRAL APPROACHES

The Method of Moments (MoM) is a way to solve integral-equations for EM fields in discretized form. The basic principles of this method are as follows:

1) The unknowns correspond to equivalent electric and equivalent magnetic surface currents ($\vec{J}$ and $\vec{M}$) at every interface, Fig. 2. Those are simply related to, respectively, the magnetic and electric fields ($\vec{H}$ and $\vec{E}$) as follows:

$$\vec{J} = \hat{n} \times \vec{H} \quad \text{and} \quad \vec{M} = -\hat{n} \times \vec{E} \tag{1}$$

Where $\hat{n}$ is the outgoing normal to the interface.

2) The equivalent currents are approximated as a superimposition of elementary basis functions, such as RWG functions [12]. For instance, the equivalent electrical current, with known basis functions $\vec{J}_i$, one sets:

$$\vec{J} \cong \sum_i x_i \vec{J}_i \quad , x_i \text{ is unknown} \tag{2}$$

3) The unknowns x_i are obtained by imposing the boundary conditions at the same interfaces. In two words, in each homogeneous domain, the fields radiated by the equivalent sources are computed and one imposes the continuity of the total tangential $\vec{E}$ and $\vec{H}$ fields at the interfaces (or "boundaries") [13]. For instance, the boundary conditions for the tangential electric field read:

$$\int_S \vec{E}_{t,1}.\vec{T}\, dS = \int_S \vec{E}_{t,2}.\vec{T}\, dS \tag{3}$$

Where $\vec{T}$ is a testing function, while indices 1 and 2 refer to fields computed on side 1 and side 2 of the interface. A similar testing is applied to the magnetic field.

4) The above principles allow one to establish a system of equations enabling the determination of the unknowns x that describe the equivalent currents. The matrix Z that describes the equations has entries that correspond to "reactions" between basis and testing functions. For instance:

$$Z_{ij} = \int_S \vec{E}\{J_j\}.\vec{J}_i ds ds' \tag{4}$$

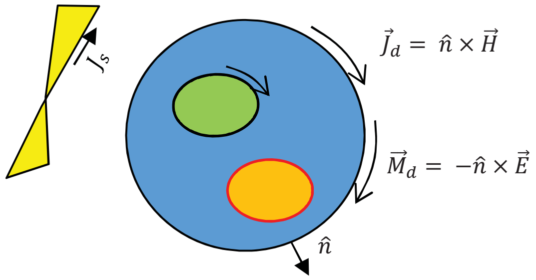

Fig. 2. Equivalent electric ($\vec{J}$) and magnetic ($\vec{M}$) currents at interfaces between homogeneous media. Left (yellow): antenna and its generator, right (blue): body with possible inclusions, at the surface of which equivalent surface currents will also be associated.

where $\vec{E}\{.\}$ is the electric field radiated by the electrical current $\vec{J}_j$. Similar entries are defined for magnetic fields and for magnetic sources (4 combinations).

III. NESTING APPROACH

In MRI once a new mesh of the antenna has been obtained, everything should rerun to compute the effect of this change in the field distribution of the desired internal organ. To avoid this, it is proposed to precompute some matrices once and for all. Here it is assumed that the body is a collection of homogeneous domains. This approach is sufficient to estimate the homogeneity of magnetic fields, as well as the maximum electric field. To this end, thanks to relatively intense pre-computations, it is possible to update the fields at the antenna level and in the body within seconds. The idea consists of avoiding re-computation of all equivalent currents inside the body everytime the antenna is modified. This is done by focusing on the equivalent currents on the outer surface of the body. It shares with [14], [15], the idea of using surface equivalence to hide details outside a given area, and using some precomputed matrices in solving integral equations [16]. Beyond this, a direct link will be established between currents on the body surface and observable fields inside any organ, though specifically defined matrices.

If x_1, x_2 and x_3 correspond to the unknowns on the antenna, on the surface of the body and on surfaces inside the body respectively, the matrix of the system of equations has the following structure:

$$\begin{bmatrix} Z_{11} & Z_{12} & 0 \\ Z_{21} & Z_{22} & Z_{23} \\ 0 & Z_{32} & Z_{33} \end{bmatrix} \tag{5}$$

Where Z_{ij} is a block of the impedance matrix that links sources on interface j and fields on interface i. The two off-diagonal zeros are due to the fact that there is no direct interaction between equivalent currents located on the antenna and on surfaces inside the body. If unknowns relative to the latter are eliminated (but not omitted), the matrix of the new system of equations reads:

$$\begin{bmatrix} Z_{11} & Z_{12} \\ Z_{21} & Z'_{22} \end{bmatrix} \tag{6}$$

Where the new matrix standing for interactions between basis functions on the surface of the body is given by:

$$Z'_{22} = Z_{22} - Z_{23}Z_{33}^{-1}Z_{32} \tag{7}$$

The fields inside the body can also be obtained by elimination from the fields on the surface of the head. By considering Fig. 1, let us now denote by x_2 the fields on the surface of the head, by x_3 the equivalent currents on the surface of the brain and by x_4 the field on all other internal organs. It is interesting to notice that there is no direct interaction between x_1 on one side and x_3 and x_4 on the other side (i.e. the corresponding matrices are zero), which simplifies calculations a little bit. Knowing that there are no sources inside the head, the corresponding interactions can be written as:

$$\begin{aligned} Z_{32}x_2 + Z_{33}x_3 + Z_{34}x_4 &= 0 \\ Z_{42}x_2 + Z_{43}x_3 + Z_{44}x_4 &= 0 \end{aligned} \tag{8}$$

From which x_3 is obtained as follows:

$$\begin{aligned} x_3 &= -(U - Z_{33}^{-1}P_{34}Z_{43})^{-1}Z_{33}^{-1}(Z_{32} - P_{34}Z_{42})x_2 \\ &= P_{32}x_2 \end{aligned} \tag{9}$$

with $P_{34} = Z_{34}Z_{44}^{-1}$

The matrix in the above equation can be computed once and for all. To obtain fields inside a given organ, one then just needs to left-multiply the currents x_3 by a matrix that provides the fields on a number of testing functions (with all three orientations) inside that organ, Let us name it Q_{30}. That matrix can directly left-multiply P_{32}. That product, denoted here as X, can also be pre-computed once and for all. Then, whenever a new value of x_2 is obtained (e.g. because the antenna design has changed), it just needs to be left-multiplied by matrix X to provide the fields inside the organ.

IV. VALIDATION

As shown in Fig. 3, a bowtie antenna is located on the XY plane below two spheres. The distance between antenna and the outer sphere is 0.2 m. The outer and inner spheres have 0.5 m and 0.25 m radius respectively. The relative permittivity for the outer sphere is 5- 0.25j and for the inner one is selected as 42-60j. The nesting approach is used here to find the electric fields inside the inner sphere. In this case, the interaction matrices between outer and inner spheres and between the inner sphere and testing functions inside the inner sphere are computed once and for all. The field distribution for the plane in the middle of spheres and parallel to the antenna is found with the method of moments and with the CST microwave studio software at 150 MHz [17]. As can be checked in Fig. 4, the results are very similar.

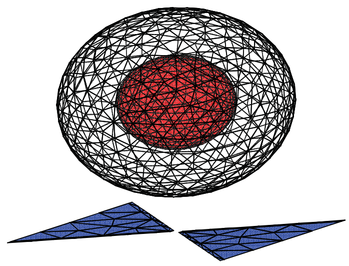

Fig. 3. A bowtie antenna is located below two spheres.

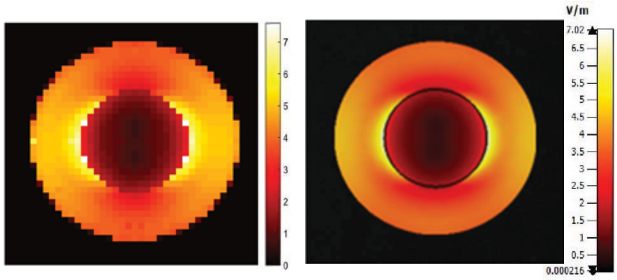

(a) Normalized E field with MOM (b) E field with CST

Fig. 4. Electric field distribution for the plane in the middle of spheres.

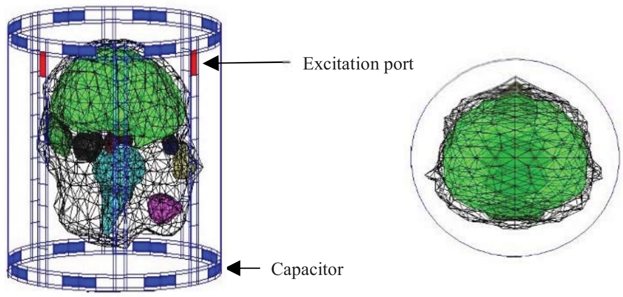

(a) Side view (b) Top view

Fig. 5. A quadrature excited birdcage antenna is located around a meshed human head with several internal organs.

In the case of MRI applications, birdcage coils through quadrature excitation and in combination with optimal value of lumped elements, provide a satisfactorily homogenous magnetic field distribution [18]. The transverse magnetic field generated by these antennas can be decomposed according to circular polarizations: the $B_1^+ = B_x + jB_y$ and $B_1^- = B_x - jB_y$ fields. The former is used for proton excitation, while the latter is used for detection of the re-emitted signal. Birdcage coils are very popular as transmit coils since the B_1^+ field can be made homogeneous over wide

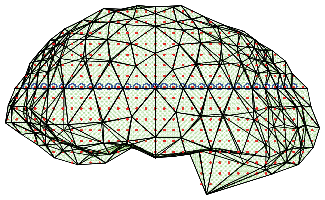

Fig. 6. Automatticaly selected 3D points inside the brain. Blue plane is the obseravtion plane of fields.

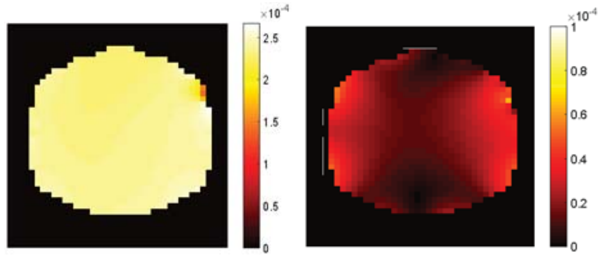

(a) Normalized B_1^+ (b) Normalized B_1^-

Fig. 7. Distribution of B_1^+ and B_1^- field inside the brain for z=3.5 cm.

volumes, while keeping the B_1^- field low. As shown in Fig. 5, a birdcage coil is excited through two ports, these two ports have 90 degrees phase shift. This kind of excitation provides homogeneous and circular polarized field distribution inside the birdcage. Depending to the configuration of lumped elements (capacitors), there are three birdcage coils types: high-pass, low-pass and hybrid. Here a high-pass birdcage antenna is used, where capacitors are located on the end rings. This coil has 8 legs, 8 cm radius, 1 cm strip width and a height of 15 cm [19], which is fit around a meshed human head. By using method of moments and equation (9), equivalent currents on the surface of the brain are obtained from the equivalent currents on the head. Using the brain mesh shown in Fig. 6, a 3D distribution of points inside the brain is given. The interaction between basis functions on the brain surface and testing functions is used to get the electric and magnetic fields inside the brain. To observe the fields inside the brain, an observation plane is selected for z equal to 3.5 cm, which is shown in Fig. 6 with blue color circles. As can be seen in Fig. 7, the B_1^+ field shows a good homogeneity in the desired plane while the B_1^- shows a low value in the same area. With the nesting approach, once a new mesh of the antenna has been obtained and its interactions matrices with the external surface of the head have been computed (this takes order of one minute), the computation time needed to renew the equivalent currents on the surface of the head is around 10 seconds. From there, obtaining the fields within the brain take only order of 1 second, thanks to the pre-computation of observation matrices. In a nutshell, one may conclude that the only significant computation time will correspond to that of the MoM matrix of the new antenna itself (which can't be avoided) and of its interaction with the external surface of the body only. Resulting surface currents and internal fields will be obtained quasi-instantly. This should remain true when the whole body is considered.

V. PERSPECTIVES

In ongoing work, we aim to develop a hybrid numerical method between the MoM and the edge-Finite Element Method (edge FEM) [20], [21]. The latter has the ability to take into account complex geometric structures and heterogeneous media, yielding an accurate and natural description of a vector field with discontinuities in 3D. In addition, the edge FEM allows a high order discretization [22], as the recent work of Bonazzoli et al. [23], providing a simple construction of high order basis functions on tetrahedral meshes. Based on the finite-element-boundary integral (FE-BI) method [24], this hybridization is intended to combine the capacity of the edge FEM to accurately deal with irregularly shaped objects and non-homogeneous materials; and the efficiency of the MoM on the rest of the computational domain, for a gain in CPU time. We also have the advantage of being able to apply a rigorous boundary condition (obtained from the MoM method) that suppresses the truncation error from absorbing boundary conditions. A further acceleration will result for precalculations based on edge FEM in order to represent, from the point of view of the outside of the body, the interactions between all basis functions at the surface of the body by a matrix, enabling the interaction of the body with the antennas, metamaterials and MRI tunnel using the MoM, while fully accounting for the details of the inside of the body.

VI. CONCLUSION

An efficient MoM approach has been proposed to find fields distributions in MRI, which significantly reduces the computation time. The approach is based on surface integral equations and assumes piecewise homogeneous organs. The idea is based on avoiding re-computation of all interactions, through a Schur complement as used in [14], [16], which consist here of interaction between internal organs and interaction between head surface and internal organs. As a result, the only matrices that appear in the final MoM formulation are those referring to the antenna and to the surface of the head. The latter accounts for the all the organs inside the head. Once the currents on the surface of the head are found, fields inside the brain are found quasi-instantly through a specific radiation matrix. A validation carried out with a commercial software showed very good results for two concentric spheres. For the MRI application, a birdcage antenna is fit around the human head, to observe the fields inside the brain. This methodology allows to typically deal with matrices of size of the order of 4000×4000 instead of 15000×15000. Supposing that a change in the MRI antenna involves a given fraction of its mesh, then the main new computation will concern the interaction between that fraction of mesh and the surface of the head, without impacting any of the matrices that deal with the fields inside the head. In further work, FEM will be used to model interactions between all basis functions on the body surface, while accounting for all the details of the inhomogeneous body. This will also allow easy link with MoM regarding antennas and metamaterials outside the body.

ACKNOWLEDGMENT

This project has received funding from the European Union Horizon 2020 research and innovation program under grant agreement No. 736937. We would also like to thank to Prof. Redha Abdeddaim from Institut Fresnel for his coordinating activity.

REFERENCES

[1] F. Bloch, W. W. Hansen, and M. Packard, "Nuclear Induction," Phys. Rev., vol. 69, p. 127, 1946.
[2] E. M. Purcell, H. C. Torrey, and R. Pound, "Resonance absorption by nuclear magnetic moments in a solid," Phys. Rev, vol. 69, p. 37, 1946.
[3] E. D. Becker, "A Brief History of Nuclear Magnetic Resonance," Anal.Chem, vol. 65, no. 6, p. 295302, Mar. 1993.
[4] D. S. Thylur, R. E. Jacobs, J. L. Go, A. W. Toga, and J. K. Niparko, "Ultra-high-field magnetic resonance imaging of the human inner ear at 11.7 Tesla," Otology & Neurotology; Am. Neurotol. Soc., p. 133, Jan. 2017.
[5] C. N. Chen, D. I. Hoult, V. J. Sank, "Quadrature detection coils—a further √2 improvement in sensitivity," Journal of Magnetic resonance, vol. 54, pp.324-327, 1983.
[6] R. F. Harrington, "Field Computation by Moment Method," FL:Krieger Publ, Malabar,1982.
[7] W. C. Chew, J. M. Jin, C. C. Lu, E. Michielssen and J. M .Song, "Fast solution methods in electromagnetics," IEEE Trans. Antennas Propag, vol. 45, pp. 533-543, Mar. 1997.
[8] J. M. Jin, "The Finite Element Method in Electromagnetics," John Wiley & Sons, 1993.
[9] K. S. Yee, "Numerical solution of initial boundary value problems involving Maxwell's equations in isotropic media," IEEE Trans. Antennas Propag, vol. 14, pp. 302–307, May 1966.
[10] A. Taflove, "Computational Electrodynamics: The Finite-Difference Time-Domain Method," Artech House, Boston, MA, 1995.
[11] I. P. Georgakis, I. I. Giannakopoulos, M.S. Litsarev, A.G. Polimeridis. "A fast volume integral equation solver with linear basis functions for the accurate computation of electromagnetic fields in MRI," arXiv preprint arXiv: 1902.02196, Feb 2019.
[12] S. Rao, D. Wilton and A. Glisson, "Electromagnetic scattering by surfaces of arbitrary shape,'' IEEE Trans. Antennas Propag, vol. 30, pp. 409–418, Mar. 1982.
[13] S. Rao and D. Wilton, "E- field, H- field, and combined field solution for arbitrarily shaped three- dimensional dielectric bodies,'' Electromagnetics, vol.10, no.4, pp. 407–421, 1990.
[14] A.M. Van de Water, B. P. de Hon, M. C. van Beurden, A. G. Tijhuis, and P. de Maagt, "Linear embedding via Green's operators: a modeling technique for finite electromagnetic band- gap structures,'' Phys. Rev. E, vol. 72, 056704, Nov. 2005.
[15] M. K. Li, W. C. Chew, "Wave-field interaction with complex structures using equivalence principle algorithm,'' IEEE Trans. Antennas Propag, vol. 55, no. 1, pp. 130-138, 2007.
[16] A.A Kucharski, "Efficient solution of integral-equation based electromagnetic problems with the use of macromodels,'' IEEE Transactions on Antennas and Propagation, vol. 56, no. 5, pp. 1482-1487, 2008.
[17] CST studio suite 2017, CST-computer simulation technology AG.
[18] C. E. Hayes, W. A. Edelstein, J. F. Schenck, O.M. Mueller and M. Eash, "An efficient, highly homogeneous radiofrequency coil for whole-body NMR imaging at 1.5 T," Journal of Magnetic Resonance, vol. 63, Issue 3, pp. 622-628, Jul. 1985.
[19] JI. Echeveste, D. Tihon, M. Dubois, R. Abdeddaim, S. Enoch, C. Craeye, "Efficient and full-wave electromagnetic analysis of MRI antennas using the Array Scanning Method,", Eucap 2018, London, Apr. 2018.
[20] J.-C. Nedelec, "A new family of mixed finite elements in R3,'' Numer. Math., vol. 50, pp. 57-81, 1986.
[21] J. P. Webb, "Hierarchical vector basis functions of arbitrary order for triangular and tetrahedral finite elements,'' IEEE Trans. Antennas Propag., vol. 47, pp. 1244–1253, 1999.
[22] F. Rapetti, A. Bossavit, "Whitney Forms of Higher Degree,'' SIAM J. Numerical Analysis, vol. 47, pp. 2369–2386, 2009.
[23] M. Bonazzoli, V. Dolean, F. Hecht, F. Rapetti, "An example of explicit implementation strategy and preconditioning for the high order edge finite elements applied to the time-harmonic Maxwell's equation,'' Computers & Mathematics with Applications, vol. 75, pp. 1498–1514, 2018.
[24] J. Guan, S. Yan, J.-M. Jin, "An accurate and efficient finite elementboundary integral method with GPU acceleration for 3-D electromagnetic analysis,'' Trans. Antennas Propag., vol. 62, pp. 6325–6336, 2014.